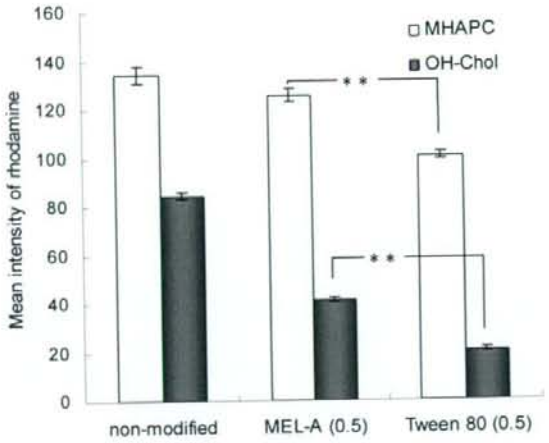

Fig.17. T Cellular association of MHAPC- and OH-Chol-lipoplex in A549 cells incubated for 2 h in PBS.

別添4
厚生科学研究費補助金 （医薬品・医療機器等レギュラトリーサイエンス総合研究事業）
分担研究報告書

プラスミドDNA/リポソームの表面状態と遺伝子発現効率

分担研究者　米谷芳枝　星薬科大学　医薬品化学研究所　教授

遺伝子導入用リポソーム製剤は、安全性は高いが遺伝子導入効率が低いのが問題となっている。遺伝子導入効率を改善するために、リポソームの表面の改質を行い、肺への遺伝子導入効率と細胞への取り込みに対するリポソームの表面状態の影響について検討した。表面の改質には、非イオン性界面活性剤としてmannosylerythritol (MEL-A)とTween 80を用いた。MEL-Aは*in vitro*と*in vivo*でともに発現を上昇したが、Tween 80はいずれにおいても上昇しなかった。リポプレックスの表面電位においては、MEL-Aは変化しないがTween 80は有意に低下させ、また、リポプレックスの表面の水和状態においては、Tween 80はMEL-Aより水和させることが明らかになった。したがって、リポプレックスの高いカチオン性の表面電位と水和状態が、細胞内取り込みに関係することが推察された。

A．研究目的

現在、遺伝子導入用リポソームベクターは安全性は高いが、遺伝子導入効率が低いのが問題となっている。遺伝子導入効率を改善するために、本研究は、肺への遺伝子送達用非ウイルスベクターの開発を目的として、カチオン性コレステロール誘導体に着目し、新規誘導体を合成し、微粒子ベクターとして*in vitro*とマウスの経肺投与における遺伝子導入効率について検討した。さらに、導入効率の改善のためにリポソームの表面の改質を行い、遺伝子導入効率と細胞への取り込みに対する影響について検討した。表面の改質には、非イオン性界面活性剤としてバイオ界面活性剤であるmannosylerythritol (MEL-A)とTween 80を用いた(Fig. 1)。

これまではリポプレックスの表面電位が遺伝子導入細胞との相互作用の指標として用いられてきたが、本研究では新たにリポソームの表面の水和状態やpHについて検討した。その結果、リポソームとプラスミドDNAとの複合体であるリポプレックスの高いカチオン性の表面電位と脱水和状態が、細胞内取り込みと遺伝子発現に関係することが推察された。

本年度は（1）非イオン性界面活性剤修飾リポソームとプラスミドDNA(DNA)からなるリポプレックスの表面の水和状態やpHが細胞取り込みに与える影響と、（2）これらリポソーム製剤によるin vivoでの遺伝子導入効率を調べた。

B．研究方法

カチオン性コレステロール誘導体（CCDs）合成

4種類の生体分解性カチオン性コレステロール誘導体（CCDs）を合成した(Fig. 1)。これらは、第一から三級のアミノ基、末端の水酸基の有無、コレステロールとのカーバメイトとアミド結合（OH-Chol）が異なっている。

リポソーム製剤による遺伝子導入実験

各CCD脂質とDOPE（モル比で1:1）からなるリポソームを修正エタノール注入法で調製した。または、MHAPCとDOPEとMEL-A、Tween 80がモル比で1:1:0.5のリポソームを同様に調製した。DNAとしては、ルシフェラーゼをコードしたプラスミドDNA pCMV-lucを用いた。カチオン性リポソームとDNAの(+/-)荷電比は3/1、5/1として水中で複合体（リポソーム/DNA、リポプレックス）を調製した。これらをA549細胞、または、

マウスの気管に内径 5 μm の注射針の注射筒を用いて肺に投与した。遺伝子導入効率は、1 ウエルあたり 2 μg DNA となるようにリポプレックスを添加して、24 時間 10%FBS 含有培地でインキュベーションし、ルシフェラーゼ発現量をピカジーンを用いて測定した。

リポプレックスの物性測定

DNAと各リポソームとの相互作用をDNAの円二色性CD測定で調べた。リポプレックスの表面のｐHは4-heptadesyl-7-hydroxycoumarin (HC) を添加したリポソームを用いて、Em300-400 nm、Ex450nm、25℃での蛍光を測定して求めた。リポプレックスの表面の水和状態は 6-dodecanoyl-2-demethylaminonaphthalene (laurdan)を添加したリポソームを用いて、25℃でEx340nmおけるEm440と490 nmでの蛍光強度の差からGP (generalized polarization) 値を求めた。

$$GP(Ex_{340}) = (I_{440} - I_{490})/(I_{440} + I_{490})$$

C．研究結果

CCDsからなるリポソームベクターを用いて *in vitro* と、マウスの肺に遺伝子投与後の導入効率とその化学構造の関連性について検討した。*in vitro* での DNA 導入効率を調べた結果、CCDs のアミノ基の末端に水酸基がない誘導体からなるリポソームが高い発現効率を示した。続いてマウスの経肺投与による遺伝子導入についても検討した結果、*in vitro* と異なり、水酸基をもつ第三級アミン誘導体（MHAPC）が導入に有効であった(Fig. 2)。

次に遺伝子導入効率を改善するために、非イオン性界面活性剤によるリポソームの表面修飾を検討した。MHAPC リポソームに MEL-A、または Tween 80 で修飾したベクターにおいて、MEL-A は *in vitro* と *in vivo* でともに発現を上昇したが、Tween 80 はいずれにおいても上昇しなかった(Fig. 2,3)。MEL-A リポソームベクターは、Tween 80 リポソームベクターに比べ、*in vitro* では細胞内に取り込まれた後 DNA を早く放出し、*in vivo* ではマウスの肺粘膜上にリポプレックスを長く保持することが確認された。

さらに、MEL-A のリポソームに対する影響をリポプレックス表面の物理化学的性質に基づいて検討した。これまではリポプレックスの表面電位が細胞との相互作用の指標として用いられてきたが、表面の水和状態やｐH について検討した。HC の解離状態からリポソーム表面の pHを、laurdanのGP値から水和状態を算出した(Fig. 4)。なお、GP 値が高いとき、水和されていることを示す。その結果、MEL-A はリポプレックスの表面電位に影響しないが、Tween 80 は有意に低下させることが明らかになった(Fig. 5)。また、Tween 80 はMEL-A よりリポプレックスのGP 値を減少させたので表面を水和させることも明らかになった(Fig. 6)。なお、このとき各リポソームと DNA の相互作用は CD 測定からはほぼ変わらず、また、表面のｐHには大きな違いはみられなかった(Fig. 7,8)。これらのリポプレックスでは、MEL-A は細胞内取り込みが変わらず、Tween 80 では減少させた (Fig. 9)。

D．考察

遺伝子導入用リポソームベクターでは、カチオン性脂質が用いられている。これはアニオン性の DNA と複合体リポプレックスを作り、なおかつアニオン性電荷をもつ細胞との相互作用をさせるために、カチオン性リポソームと DNA の(+/-)荷電比を調整してカチオン性になるようにしている。従って、このカチオン性脂質の設計は遺伝子導入の鍵となる。また、リポプレックスになったとき、DNA とリポソーム脂質膜との強い分子的相互作用により、サイズや表面状態が変化することが知られている。そのため、これまではリポプレックスの表面状態は表面電位の測定で評価されてきたが、ここでは新たに表面の水和状態と pH が細胞取り込みや遺伝子導入効率の指標にならないかを検討した。

まず、新規カチオン性脂質としては、生体分解性が高く、DNA と適度に相互作用をする脂質として、4 種類の生体分解性コレステロール誘導体（CCD s）を合成した。これらは第一から三級のアミノ基、末端の水酸基の有無、コレステロールとの結合がカーバメイトとアミド結合（OH-Chol）と異なっている。

in vitro と *in vivo* での遺伝子導入に有効な CCD は異なり、*in vivo* では水酸基をもつ第三級アミンをもつ MHAPC が導入に有効であったことから、肺粘膜上では第三級アミンによるプラスミド DNA との強い結合が DNA の安定性に必要と考えられた。

リポソームの表面状態の遺伝子導入効率と細胞への取り込みに対する影響について検討した。リポソーム表面の改質に用いた MEL-A は *in vitro* と *in vivo* でともに発現を上昇したが、Tween 80 はいずれにおいても上昇しなかった。リポプレックスの表面電位においては、MEL-A は変化しないが Tween 80 は有意に低下させ、また、リポプレックスの表面の水和状態においては、Tween 80 は MEL-A より水和させることが明らかになった。したがって、リポプレックスの高いカチオン性の表面電位と水和状態が、細胞内取り込みに関係すると推察された。さらに、MEL-A リポソームベクターは、Tween 80 リポソームベクターに比べ、*in vitro* では細胞に取り込まれた後 DNA を早く放出したことより、MEL-A は Tween 80 リポソームベクターと異なる細胞取り込み機構を誘導する可能性が示唆された。

E．結論

本研究の結果より、遺伝子導入用リポソーム製剤には、リポソーム/DNA 複合体の高いカチオン性の表面電位と水和状態が、細胞内取り込みに関係すると推察された。今後のリポソームベクターの遺伝子導入効率を予見するうえでの 1 つのマーカーとして、リポソームの表面水和状態を使用できる可能性が示唆された。

F．健康危険情報

なし

G．研究発表

1. 論文発表

1) H.L. Ma, X.R. Qi, W.X. Ding, Y. Maitani, T. Nagai. Magnetic targeting after femoral artery administration and biocompatibility assessment of superparamagnetic iron oxide nanoparticles. *J Biomed Mater Res A.* 84A(3):598-606 (2008)
2) A. Hayama, T. Yamamoto, M. Yokoyama, K. Kawano, Y. Hattori, Y. Maitani. Polymeric micelles modified by folate-PEG-lipid for targeted drug delivery to cancer cells in vitro. *J Nanosci Nanotechnol.,* 8:3085-3090 (2008)
3) N. Takahashi, Y. Watanabe, Y. Maitani, T. Yamauchi, K. Higashiyama, T. Ohba. p-dodecylaminophenol derived from the synthetic retinoid, fenretinide: Antitumor efficacy in vitro and in vivo against human prostate cancer and mechanism of action. *Int J Cancer.* 122(3):689-98 (2008)
4) W. Ding, Y. Hattori, K. Higashiyama, Y. Maitani. Hydroxyethylated cationic cholesterol derivatives in liposome vectors promote gene expression in the lung. *Int. J. Pharm.*, 354(1-2):196-203 (2008)
5) M. Furuhata, R. Danev, K. Nagayama, Y. Yamada, H. Kawakami, K. Toma, Y.Hattori, Y. Maitani. Decaarginine-PEG-artificial lipid/DNA complex for gene delivery: nanostructure and transfection efficiency, *J Nanosci Nanotechnol.,* 8 (5), 2308-315 (2008)
6) Y. Maitani , Y. Aso , A. Yamada, S. Yoshioka. Effect of sugars on storage stability of lyophilized liposome /DNA complexes with high transfection efficiency, *Int. J. Pharm.*, 356:69-75 (2008)
7) K. Niikura, Y. Kobayashi, D. Okutsu, M. Furuya, K. Kawano, Y. Maitani, T. Suzuki, M. Narita. Implication of spinal protein kinase Cgamma isoform in activation of the mouse brain by intrathecal injection of the protein kinase C activator phorbol 12,13-dibutyrate using functional magnetic resonance imaging analysis. *Neurosci Lett.*, 433(1):6-10 (2008)
8) H.L. Ma, Y.F. Xu, X.R. Qi, Y. Maitani, T. Nagai. Superparamagnetic iron oxide

nanoparticles stabilized by alginate: Pharmacokinetics, tissue distribution, and applications in detecting liver cancers. *Int J Pharm.* 354(1-2):217-26 (2008)
9) Y. Maitani, S. Katayama, K. Kawano, A. Hayama, K. Toma, Artificial Lipids Stabilized Camptothecin Incorporated into Liposomes *Biol. Pharm. Bull.*, 31(5), 990-993, (2008)
10) M. Watanabe, K. Kawano, K.Toma, Y. Hattori, Y. Maitani, In vivo antitumor activity of camptothecin incorporated in liposomes formulated with an artificial lipid and human serum albumin, *J. Control. Release,* 127 231–238 (2008)
11) T. Fujita, M. Furuhata, Y. Hattori, H. Kawakami, K. Toma, Y. Maitani, High gene delivery in tumor by intratumoral injection of tetraarginine-PEG lipid-coated protamine/DNA, *J. Control. Release,* 129(2)124-127 (2008)
12) Y. Ohguchi, K. Kawano, Y. Hattori, Y. Maitani, Selective delivery of folate-PEG-linked nanoemulsion-loaded aclacinomycin A to KB nasopharyngeal cells and xenograft: Effect of chain length and amount of folate-PEG linker, *J. Drug Targeting,* 16(9), 660-667 (2008)
13) A.Yamada, Y. Taniguchi, K. Kawano, T. Honda, Y. Hattori, Y. Maitani, Design of folate-linked liposomal doxorubicin to its antitumor effect in mice, *Clinical Cancer Res,* 14 (24) 8161-8168(2008)
14) T. Yoshizawa, Y. Hattori, M. Hakoshima, K. Koga and Y. Maitani, Folate-linked lipid-based nanoparticles for synthetic siRNA delivery in KB tumor xenografts, *European Journal of Pharmaceutics and Biopharmaceutics*, 70, 718-725 (2008)
15) Y. Hattori, T. Yoshizawa, K. Koga, Y. Maitani, NaCl induced high cationic hydroxyethylated cholesterol-based nanoparticle-mediated synthetic siRNA transfer into prostate carcinoma PC-3 cells, *Biol. Pharm. Bull.* 31. 2294-2301 (2008)
16) T. Fujita, M. Furuhata, Y. Hattori, H. Kawakami, K. Toma, Y. Maitani, Calcium enhanced delivery of tetraarginine-PEG-lipid-coated DNA/protamine complexes, *Int J Pharm.* 368, 186-192 (2009)
17) W. Ding, T. Izumisawa, Y. Hattori, X. Qi, D. Kitamoto, Y. Maitani, Non-ionic surfactant modified cationic liposomes mediated gene transfection in vitro and in the mouse lung, Biol. Pharm. Bull. 32(2):311-315 (2009)
18) K. Kawano, E. Onose, Y. Hattori, Y. Maitani, Higher liposomal membrane fluidity enhances the in vitro anti-tumor activity of folate-targeted liposomal mitoxantrone, Molecular Pharmaceutics, 6(1), 98-104 (2009).
19) W. Ding, Y. Hattori, X. Qi, D. Kitamoto, Y. Maitani, Surface properties of lipoplexes modified with MEL-A and Tween 80, Chem. Pharm. Bull. 57(2), 138-143 (2009)
20) Y. Hattori, L. Shi, W. Ding, K. Koga, K. Kawano, M. Hakoshima, Y. Maitani, Novel irinotecan-loaded liposome using phytic acid with high therapeutic efficacy for colon tumors, *J. Control. Release,* in press.
21) Y. Hattori, K. Koga, T. Izumisawa, M. Yamasaki, R. Narishima, S. Yoshida, T. Fukui, Y. Maitani, The distribution of mRNA expression and protein after hydrodynamic injection of transgene in mice, *Biol. Pharm. Bull.* in press.
22) M. Furuhata, T. Izumisawa, H. Kawakami, K. Toma, Y. Hattori, Y. Maitani, Decaarginine-PEG-liposome Enhanced Transfection Efficiency and Function of Arginine Length and PEG, *Int J Pharm.* in press.
23) Y. Li, X. R. Qi , Y. Maitani, T. Nagai, PEG-PLA diblock copolymer micelle-like nanoparticles as all-trans-retinoic acid carrier: in vitro and in vivo characterizations, Nanotechnology, in press.

2. 学会発表

1) 箕輪卓也、川野久美、白石貢一、横山昌幸、米谷芳枝、Gd 封入リポソーム製剤の MRI による腫瘍集積性の評価、フィジカル・ファーマフォーラム、2008.3.24-25
2) 下條裕樹、渡辺和男、箕輪潤一、梅田 勲、川野久美、服部喜之、米谷芳枝、Layer-by-Layer 法を用いた表面修飾リポソーム製剤の放出性評価、フィジカル・ファーマフォーラム、2008.3.24-25
3) 萩原彩子、服部喜之、丁武孝、米谷芳枝、正電荷コレステロール誘導体を用いた siRNA 送達用脂質ナノ粒子の開発、日本薬学会 第 128 年会、2008.3.26-28
4) 施力、服部喜之、丁武孝、古賀公子、箱島基貴、川野久美、米谷芳枝、フィチン酸を用いたイリノテカン封入リポソーム製剤の調製と抗腫瘍効果の評価、日本薬学会 第 128 年会、2008.3.26-28

5) 古賀公子、服部喜之、米谷芳枝、悪性内分泌腫瘍における RET 標的 siRNA と抗癌剤の併用治療、日本薬学会 第 128 年会、2008.3.26-28
6) 日置敦子、川野久美、服部喜之、米谷芳枝、血中滞留性リポソーム製剤の in vitro 放出性、日本薬学会 第 128 年会、2008.3.26-28
7) 小野瀬絵里、川野久美、服部喜之、米谷芳枝、葉酸修飾リポソームの抗腫瘍効果における脂質膜組成の影響、日本薬学会 第 128 年会、2008.3.26-28
8) 古幡昌彦、川上宏子、戸澗一孔、米谷芳枝、オリゴアルギニン PEG 修飾リポソームによる細胞内取り込み経路および遺伝子発現、日本薬学会 第 128 年会、2008.3.26-28
9) 下條裕樹、渡辺和男、箕輪潤一、梅田勲、川野久美、服部喜之、米谷芳枝、Layer-by-Layer 法を用いた表面修飾リポソーム製剤の調製と評価、日本薬学会 第 128 年会、2008.3.26-28
10) 小林昇平、古幡昌彦、R. Danev、永山國昭、戸澗一孔、服部喜之、米谷芳枝、原口徳子、オリゴアルギニン脂質／DNA 複合体の細胞内動態、遺伝子・デリバリー研究会 第 8 回シンポジウム、2008.5.9
11) 古賀公子、服部喜之、福島正義、米谷芳枝、ハイドロダイナミクス法を用いたアディポネクチン遺伝子による糖尿病遺伝子治療、日本薬剤学会 第 23 年会、2008. 5.20-22
12) 箕輪卓也、川野久美、白石貢一、横山昌幸、米谷芳枝、Gd 封入リポソームの DCE-MRI による腫瘍血管透過性の評価、第 3 回日本分子イメージング学会学術大会、 2008.5.22-23
13) 丁武孝、服部喜之、米谷芳枝、MEL-A modified MHAPC-liposomes for gene delivery in vitro and in the lung、第 10 回応用薬理シンポジウム、2008.6.7-8
14) 谷口幸覧、川野久美、米谷芳枝、葉酸と PEG 修飾のデザインによるドキソルビシン封入リポソーム製剤の抗腫瘍効果の評価、第 24 回日本 DDS 学会、2008. 6. 29-30
15) Xian Rong Qi , Yuan Li, Yoshie Maitani, Tsuneji Nagai, PEG-PLA diblock copolymer micelle-like nanoparticles as all-trans-retinoic acid carrier: in vitro and in vivo characterizations, 第 24 回日本 DDS 学会、2008. 6. 29-30
16) 箕輪卓也、川野久美、白石貢一、横山昌幸 、米谷芳枝、Gd 封入リポソーム製剤の MRI による腫瘍集積性の評価、第 24 回日本 DDS 学会、2008. 6. 29-30
17) 箱島 基貴、服部 喜之、米谷 芳枝、Her-2 発現腫瘍に対する Her-2 標的 siRNA と抗癌剤との併用治療の検討、第 24 回日本 DDS 学会、2008. 6. 29-30
18) Y. Hattori and Y. Maitani, Cationic Hydroxyethylated Cholesterol-based Nanoparticle-Mediated Synthetic siRNA Transfer into Prostate Carcinoma PC-3 Cells, 11th LIPOSOME RESEARCH DAYS CONFERENCE, 2008.7.19-22
19) Y. Taniguchi, K. Kawano, Y. Maitani, Targeting effect of folate-linked liposomal doxorubicin was improved by TGF-β inhibitor, 11th LIPOSOME RESEARCH DAYS CONFERENCE, 2008.7.19-22
20) K. Koga, Y. Hattori, Y. Maitani, RET-targeted siRNA Inhibits the Growth in Medullary Thyroid Carcinoma TT Cells and the Xenografts, 11th LIPOSOME RESEARCH DAYS CONFERENCE, 2008.7.19-22
21) 丁武孝、泉澤友宏、服部喜之、米谷芳枝, MEL-A and Tween 80 modified cationic liposomes for gene transfection in vitro and in the lung, 11th LIPOSOME RESEARCH DAYS CONFERENCE, 2008.7.19-22
22) Y. Maitani, A.Yamada, Y. Taniguchi, K. Kawano, Y. Hattori, Design of folate linked-liposomal doxorubicin to its antitumor effect in mice, Ehrlich II, 2nd World Conference on Magic Bullets, 2008.10.3-5
23) Y. Maitani, Liposomal Drug Delivery : An Update, 22nd Federation of Asian Pharmaceutical Association Congress, 2008. 11.7-10

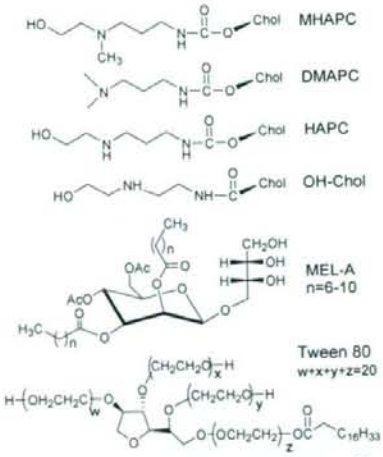

Fig. 1 Chemical structures of cationic lipids and surfactants

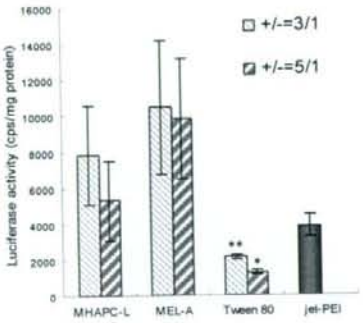

Fig.2 Gene transfections of MHAPC-lipoplexes in the lung at 24 h

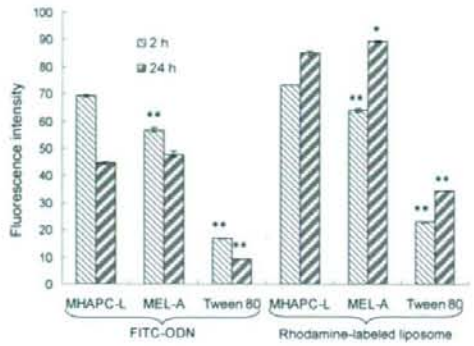

Fig.3 Cellular association of MHAPC-lipoplexes (+/-=3/1) in A549 cells.

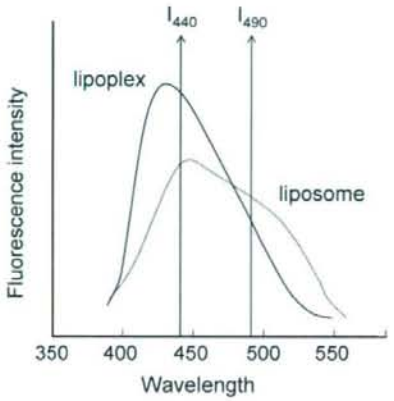

Fig. 4 The representative spectrum of laurdan in liposome and lipoplex

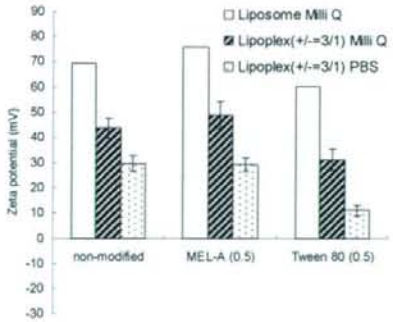

Fig. 5 ζ-potential of MHAPC-liposome and –lipoplex in Milli Q and PBS.

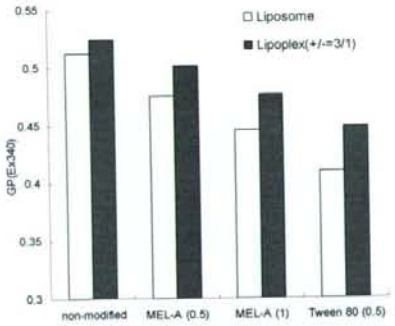

Fig.6 Change of GP values (hydration) of MHAPC-liposome and –lipoplex.

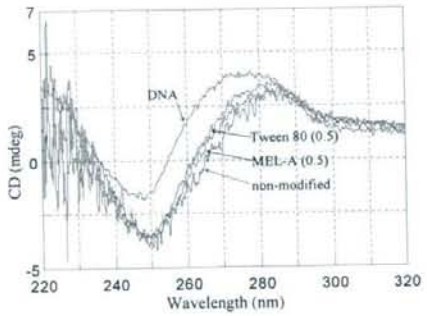

Fig.7 The CD spectrum of DNA in MHAPC-lipoplex.

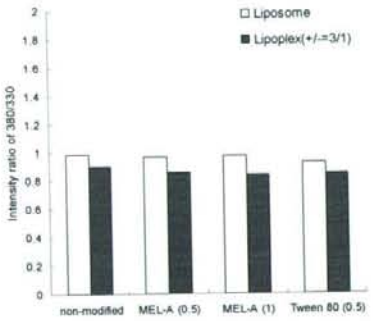

Fig.8 Change of surface pH of MHAPC-liposome and –lipoplex.

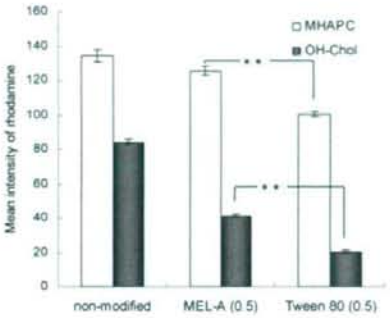

Fig. 9 Cellular association of MHAPC- and OH-Chol-lipoplex in A549 cells incubated for 2 h in PBS.

別添５

研究成果の刊行に関する一覧表

雑誌

発表者氏名	論文タイトル名	発表誌名	巻号	ページ	出版年
Aso, Y., Yoshioka, S., Miyazaki, T., Kawanishi, T	Feasibility of ^{19}F-NMR for assessing the molecular mobility of flufenamic acid in solid dispersions.	*Chem. Pharm. Bull.*	57	61-64	2009
Yoshioka, S., Aso, Y., Kawanishi, T	Wide-Ranging Molecular Mobilities of Water in Active Pharmaceutical Ingredient (API) Hydrates as Determined by NMR Relaxation Times	*J Pharm. Sci.*	97	4258-4268	2008
W. Ding, Y. Hattori, K. Higashiyama, Y. Maitani	Hydroxyethylated cationic cholesterol derivatives in liposome vectors promote gene expression in the lung	*Int. J. Pharm*	354(1-2)	196-203	2008
M. Furuhata, R. Danev, K. Nagayama, Y. Yamada, H. Kawakami, K. Toma, Y.Hattori, Y. Maitani.	Decaarginine-PEG-artificial lipid/DNA complex for gene delivery: nanostructure and transfection efficiency	*J Nanosci Nanotechnol*	8 (5)	2308-315	2008
Y. Maitani , Y. Aso , A. Yamada, S. Yoshioka.	Effect of sugars on storage stability of lyophilized liposome /DNA complexes with high transfection efficiency	*Int. J. Pharm*	356	69-75	2008
Y. Maitani, S. Katayama, K. Kawano, A. Hayama, K. Toma	Artificial Lipids Stabilized Camptothecin Incorporated into Liposomes	*Biol. Pharm. Bull.*	31(5)	990-993	2008

M. Watanabe, K. Kawano, K.Toma, Y. Hattori, Y. Maitani	In vivo antitumor activity of camptothecin incorporated in liposomes formulated with an artificial lipid and human serum albumin	*J. Control. Release*	127	231–238	2008
T. Fujita, M. Furuhata, Y. Hattori, H. Kawakami, K. Toma, Y. Maitani	High gene delivery in tumor by intratumoral injection of tetraarginine-PEG lipid-coated protamine/DNA	*J. Control. Release*	129(2)	124-127	2008
T. Yoshizawa, Y. Hattori, M. Hakoshima, K. Koga and Y. Maitani,	Folate-linked lipid-based nanoparticles for synthetic siRNA delivery in KB tumor xenografts	*European Journal of Pharmaceutics and Biopharmaceutics*	70	718-725	2008
Y. Hattori, T. Yoshizawa, K. Koga, Y. Maitani	NaCl induced high cationic hydroxyethylated cholesterol-based nanoparticle-mediated synthetic siRNA transfer into prostate carcinoma PC-3 cells	*Biol. Pharm. Bull.*	31	2294-2301	2008
T. Fujita, M. Furuhata, Y. Hattori, H. Kawakami, K. Toma, Y. Maitani	Calcium enhanced delivery of tetraarginine-PEG-lipid-coated DNA/protamine complexes	*Int J Pharm*	368,	186-192	2009
W. Ding, T. Izumisawa, Y. Hattori, X. Qi, D. Kitamoto, Y. Maitani	Non-ionic surfactant modified cationic liposomes mediated gene transfection in vitro and in the mouse lung	*Biol. Pharm. Bull.*	32(2)	311-315	2009
W. Ding, Y. Hattori, X. Qi, D. Kitamoto, Y. Maitani	Surface properties of lipoplexes modified with MEL-A and Tween80	*Chem. Pharm. Bull.*	57(2)	138-143	2009

Y. Hattori, L. Shi, W. Ding, K. Koga, K. Kawano, M. Hakoshima, Y. Maitani	Novel irinotecan-loaded liposome using phytic acid with high therapeutic efficacy for colon tumors	*J. Control. Release*		in press	2009
Y. Hattori, K. Koga, T. Izumisawa, M. Yamasaki, R. Narishima, S. Yoshida, T. Fukui, Y. Maitani,	The distribution of mRNA expression and protein after hydrodynamic injection of transgene in mice, Biol. Pharm. Bull. in press.	*Int J Pharm.*		in press.	2009
M. Furuhata, T. Izumisawa, H. Kawakami, K. Toma, Y. Hattori, Y. Maitani,	Decaarginine-PEG-liposome Enhanced Transfection Efficiency and Function of Arginine Length and PEG	*Int J Pharm.*		in press.	2009
Y. Li, X. R. Qi , Y. Maitani, T. Nagai,	PEG-PLA diblock copolymer micelle-like nanoparticles as all-trans-retinoic acid carrier: in vitro and in vivo characterizations,	Nanotechnology,		in press.	2009

研究成果の刊行物・別刷

Feasibility of ^{19}F-NMR for Assessing the Molecular Mobility of Flufenamic Acid in Solid Dispersions

Yukio Aso,* Sumie Yoshioka, Tamaki Miyazaki, and Toru Kawanishi

National Institute of Health Sciences; 1–18–1 Kamiyoga, Setagaya, Tokyo 158–8501, Japan.
Received September 9, 2008; accepted October 22, 2008; published online October 23, 2008

The purpose of the present study was to clarify the feasibility of ^{19}F-NMR for assessing the molecular mobility of flufenamic acid (FLF) in solid dispersions. Amorphous solid dispersions of FLF containing poly(vinylpyrrolidone) (PVP) or hydroxypropylmethylcellulose (HPMC) were prepared by melting and rapid cooling. Spin–lattice relaxation times (T_1 and $T_{1\rho}$) of FLF fluorine atoms in the solid dispersions were determined at various temperatures (−20 to 150 °C). Correlation time (τ_c), which is a measure of rotational molecular mobility, was calculated from the observed T_1 or $T_{1\rho}$ value and that of the T_1 or $T_{1\rho}$ minimum, assuming that the relaxation mechanism of spin–lattice relaxation of FLF fluorine atoms does not change with temperature. The τ_c value for solid dispersions containing 20% PVP was 2—3 times longer than that for solid dispersions containing 20% HPMC at 50 °C, indicating that the molecular mobility of FLF in solid dispersions containing 20% PVP was lower than that in solid dispersions containing 20% HPMC. The amount of amorphous FLF remaining in the solid dispersions stored at 60 °C was successfully estimated by analyzing the solid echo signals of FLF fluorine atoms, and it was possible to follow the overall crystallization of amorphous FLF in the solid dispersions. The solid dispersion containing 20% PVP was more stable than that containing 20% HPMC. The difference in stability between solid dispersions containing PVP and HPMC is considered due to the difference in molecular mobility as determined by τ_c. The molecular mobility determined by ^{19}F-NMR seems to be a useful measure for assessing the stability of drugs containing fluorine atoms in amorphous solid dispersions.

Key words ^{19}F-NMR; molecular mobility; stability; crystallization; solid dispersion

Amorphous solid dispersions are used for improving the dissolution rate and solubility of poorly soluble drugs. However, drugs in amorphous form are generally less stable than crystalline drugs because of their higher energy state and higher molecular mobility. It is well known that polymeric excipients can reduce the crystallization rate of many amorphous drugs.[1—12] This stabilization by poly(vinylpyrrolidone) (PVP) is partly attributable to its ability to decrease molecular mobility, as indicated by increases in the glass transition temperature (T_g).[9] Therefore, it is of great interest to estimate the molecular mobility of drugs in solid dispersions. Although ^{13}C-NMR relaxation measurements are useful for assessing the molecular mobility of drugs in solid dispersions,[13] the low sensitivity of ^{13}C because of its low natural abundance is a drawback of ^{13}C-NMR. In contrast to ^{13}C, ^{19}F has very favorable sensitivity in NMR experiments, since it is present in 100% natural abundance, is second only to the proton in its resonance frequency (except ^{3}H) and has a spin quantum number of 1/2. The receptivity for ^{19}F is 83% of that for ^{1}H and 4700 times of that for ^{13}C.[14] Many drugs containing fluorine atoms are listed in The Japanese Pharmacopoeia. In contrast, almost all pharmaceutical excipients do not contain fluorine atoms. ^{19}F-NMR may therefore have an advantage over ^{13}C-NMR or ^{1}H-NMR for selectivity and sensitivity when assessing the molecular mobility of drugs containing fluorine atoms in pharmaceutical dosage forms such as solid dispersions.

The orientations and molecular mobility of flufenamic acid (FLF)[15] and ^{19}F-labeled α-tocopherol[16] in a lipid bilayer were studied using ^{19}F-NMR. Structures and molecular mobility of ^{19}F-labeled peptides and proteins in biological membranes were also investigated.[17—20] To the authors' knowledge, application of ^{19}F-NMR to studies of drug molecular mobility in solid dispersions has not been reported. This paper describes the feasibility of ^{19}F-NMR for assessing the molecular mobility of FLF in PVP or hydroxypropylmethylcellulose (HPMC) solid dispersions, and discusses the effect of polymer excipients on the crystallization tendency of FLF in solid dispersions in terms of differences in molecular mobility.

Experimental

Materials FLF (Fig. 1) was purchased from Wako Pure Chemical Industry (Osaka), and PVP and HPMC were from Sigma (St. Louis, MO, U.S.A.). FLF solid dispersions with PVP or HPMC were prepared by melting and cooling of mixtures of FLF with PVP or HPMC. The solid dispersions obtained were confirmed to be amorphous from microscopic observation under polarized light.

Nuclear Magnetic Relaxation Measurements ^{19}F-NMR measurements were carried out using a model JNM-MU25 pulsed NMR spectrometer (JEOL DATUM, Tokyo) operating at a resonance frequency of 25 MHz. Time profiles of spin–spin relaxation of the ^{19}F atoms of FLF were measured using the "solid echo" pulse sequence to overcome the dead time of the instrument. Spin–lattice relaxation time in the laboratory frame (T_1) was measured using the inversion recovery pulse sequence. Spin–lattice relaxation time in the rotating frame ($T_{1\rho}$) was measured at spin locking intensity of 10 G.

DSC Measurements T_g of FLF-PVP and FLF-HPMC solid dispersions was measured by DSC using a model 2920 differential scanning calorimeter and a refrigerator cooling system (TA Instruments, Newcastle, DE, U.S.A.). Approximately 5 mg of each solid dispersions was put into an aluminum sample pan and then sealed hermetically. T_g was measured at a heating rate of 20 °C/min. Temperature calibration of the instrument was carried out using indium.

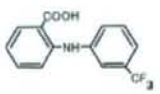

Fig. 1. Structure of FLF

* To whom correspondence should be addressed. e-mail: aso@nihs.go.jp

Results and Discussion

Molecular Mobility of FLF as Measured by ^{19}F-NMR Spin–Lattice Relaxation Time T_1 and $T_{1\rho}$ of fluorine atoms of FLF in PVP and HPMC solid dispersions were measured using a pulsed NMR spectrometer in the temperature range from −20 to 150 °C. T_1 is sensitive to the molecular motion on the time scale of the resonance frequency (MHz order). On the other hand, $T_{1\rho}$ is sensitive to the molecular motion with a frequency equivalent to the intensity of spin locking field (typically mid kHz order).[21] The temperature dependence of T_1 and $T_{1\rho}$ exhibits minimum at a specific temperature at which the molecules of interest have molecular motion with MHz time scale or mid kHz time scale predominantly. The resonance frequency of 25 MHz, lower than that of a conventional high resolution NMR spectrometer, was used to observe T_1 minimum in the temperature rage studied. Figure 2 shows the temperature dependence of T_1 and $T_{1\rho}$ of FLF fluorine atoms in PVP and HPMC solid dispersions. For FLF–PVP solid dispersions (7 : 3), the minimum of T_1 or $T_{1\rho}$ was observed at about 90 °C and 60 °C, respectively (Fig. 2A). When the PVP content decreased to 20% (w/w), T_1 and $T_{1\rho}$ of FLF at temperatures above 70 °C could not be determined due to rapid crystallization. Similar temperature dependence of T_1 or $T_{1\rho}$ was observed for the FLF–HPMC solid dispersions (Fig. 2B). The temperature difference between T_1 and $T_{1\rho}$ minimum is considered to be due to the difference in the time scale of molecular motion reflected on T_1 (MHz order) and $T_{1\rho}$ (mid kHz order). Since the molecular motion on MHz time scale becomes predominant at higher temperature than molecular motion on mid kHz time scale, T_1 minimum is observed at higher temperature than $T_{1\rho}$ minimum.

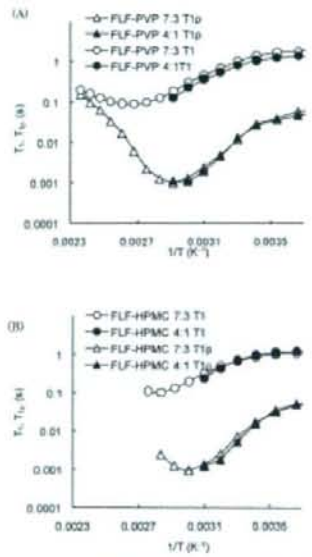

Fig. 2. Temperature Dependence of T_1 and $T_{1\rho}$ of FLF Fluorine Atoms in PVP (A) and HPMC (B) Solid Dispersions

We made following assumptions in order to estimate the molecular mobility of FLF from T_1 and $T_{1\rho}$ of FLF fluorine atoms: first, we assumed that FLF fluorine atoms in the solid dispersions relaxes mainly *via* dipolar interaction, and that the contribution of the spin–rotation interaction mechanism[21] is negligible. While relaxation *via* the spin–rotation interaction mechanism has been reported for liquid sample,[22–24] complete domination of dipolar interactions has been reported for fluorine atoms for polycrystalline van der Waals molecular solid.[25] We also made an assumption that the contribution of the cross-relaxation between fluorine and proton atoms can be considered small. It is known that relaxation is not intrinsically single-exponential when cross-relaxation between fluorine and proton atoms takes place.[14] However, we assumed small contribution of the cross-relaxation, because the relaxation of FLF fluorine atoms in the solid dispersions was exponential within experimental uncertainty. In studies of molecular motions, a large number of models describing molecular motions have been proposed for calculation of the spectrum density function.[26] We used a simple model that the molecular motion reflected on T_1 or $T_{1\rho}$ is represented by single correlation time for the purpose of comparing the mobility of FLF in the PVP and HPMC solid dispersions. According to the above assumptions, T_1 and $T_{1\rho}$ are described by Eqs. 1 and 2.[21]

$$\frac{1}{T_1} = \frac{6}{20}\frac{\gamma^4\hbar^2}{r^6}\left\{\frac{\tau_c}{1+\omega_0^2\tau_c^2} + \frac{4\tau_c}{1+4\omega_0^2\tau_c^2}\right\} \quad (1)$$

$$\frac{1}{T_{1\rho}} = \frac{3}{20}\frac{\gamma^4\hbar^2}{r^6}\left\{\frac{3\tau_c}{1+4\omega_1^2\tau_c^2} + \frac{5\tau_c}{1+\omega_0^2\tau_c^2} + \frac{2\tau_c}{1+4\omega_0^2\tau_c^2}\right\} \quad (2)$$

where τ_c is the correlation time that characterizes molecular reorientations, and ω_0 and ω_1 are the resonance frequencies of fluorine atoms in the static magnetic field and spin locking field, respectively. γ, r and $\hbar$ are the gyromagnetic ratio of fluorine, the distance of neighboring fluorine atoms, and the Plank constant divided by 2π, respectively. Equations 1 and 2 infer that T_1 and $T_{1\rho}$ become minimal when $\omega_0\tau_c$ is approximately 0.62[27] and $\omega_1\tau_c$ is approximately 0.52,[21] respectively. When the minimum of T_1 or $T_{1\rho}$ is observed, we can calculate the unknown value, r, in Eqs. 1 and 2. If r is known, the τ_c value can be calculated from the observed T_1 or $T_{1\rho}$ value, assuming that r does not change with temperature.

The values of r calculated from the T_1 and $T_{1\rho}$ minimum observed for the FLF–PVP solid dispersion (7 : 3) were 2.3 and 2.4 Å, respectively, and similar r values were obtained for the FLF–HPMC solid dispersion (7 : 3). These values are comparable to the reported value (2.174 Å) for 3-(trifluoromethyl)phenanthrene,[25] indicating that dipole interaction between neighboring fluorine atoms can be considered the predominant relaxation mechanism of FLF fluorine atoms in the solid dispersions. The difference between the r values obtained in this work and the reported value suggests that the possibility of the spin–rotation interaction mechanism and/or dipole interaction between fluorine and proton atoms cannot be excluded as a relaxation mechanism of FLF fluorine atoms.

Figure 3 shows the temperature dependence of τ_c calculated from T_1 and $T_{1\rho}$ for FLF fluorine atoms in the solid dis-

persions. The τ_c of FLF fluorine atoms in PVP solid dispersions calculated from $T_{1\rho}$ was 8.2 μs at 50 °C, which was about 3 times larger than that in HPMC solid dispersions (2.6 μs), indicating that the molecular mobility of FLF was lowered more strongly by PVP than by HPMC.

The τ_c values calculated using T_1 values differ from those calculated from $T_{1\rho}$ values. The slope of temperature dependence of τ_c changed around T_g. These findings suggest that the assumption that the molecular motion reflected on T_1 and $T_{1\rho}$ is represented by a single τ_c may be too simple to describe the molecular motion of FLF in the solid dispersions at temperatures studied, and that two or more molecular motions, such as rotation of trifluoromethyl group and motions with larger scales than rotation of trifluoromethyl group, may be reflected on T_1 and $T_{1\rho}$. Further studies including ^{1}H-NMR relaxation measurement and dielectric relaxation measurements will be needed to identify the detailed molecular motion of FLF in the solid dispersions.

Correlation between Crystallization Tendency and Molecular Mobility of FLF in Solid Dispersions Crystallization proceeds *via* formation of crystal nuclei and crystal growth. As a measure of the crystallization tendency of amorphous FLF in solid dispersions, the overall crystallization rate of amorphous FLF in the solid dispersions was estimated from the time profiles amorphous FLF remaining in the solid dispersions instead of measuring the nucleation rate and growth rate. Amorphous FLF remaining in the solid dispersions was estimated by analyzing solid echo signals of FLF fluorine atoms. Figure 4 shows the solid echo signal of fluorine atoms of FLF in solid dispersions containing 20% (w/w) PVP and that of fluorine atoms of crystalline FLF. The signal for the solid dispersions was describable by the Lorentzian relaxation equation (Eq. 3), and its relaxation time (T_{2L}) was approximately 140 μs. Crystalline FLF exhibited Gaussian relaxation signals (Eq. 4), and its relaxation time (T_{2G}) was approximately 30 μs. These results indicate that amorphous FLF in solid dispersions is considered to exhibit Lorentzian relaxation signals.

$$I = I_0 \exp(-t/T_{2L}) \tag{3}$$

$$I = I_0 \exp\{-t^2/(2T_{2G}^2)\} \tag{4}$$

where I_0 and I represent the signal intensities at time 0 and t, respectively. Figure 5 shows solid echo signals for the fluorine atoms of FLF in the solid dispersions stored at 60 °C. Samples stored at 60 °C exhibited biphasic decay signals, and signals were describable by summation of the Gaussian (solid line) and Lorentzian (dashed line) equations (Eq. 5).

$$I = I_0\{P_L \exp(-t/T_{2L}) + P_G \exp(-t^2/2T_{2G}^2)\} \tag{5}$$

where P_L and P_G are the ratio of fluorine atoms exhibiting Lorentzian and Gaussian relaxation process, respectively, and $P_L + P_G = 1$. Assuming that the T_{2L} and T_{2G} values are 140 and 30 μs, respectively, P_L values of FLF in the solid dispersions were estimated by curve fitting. P_L values of the solid dispersions decreased with increasing storage time, indicating that crystallization of amorphous FLF in solid dispersions takes place during storage at 60 °C. To certify the reliability of the P_L values obtained by ^{19}F-NMR measurements, change in the heat capacity at T_g ($\Delta C_p(T_g)$) was determined for the solid dispersions stored at 60 °C for various periods as a measure of amorphous FLF remaining, and was compared with the value of P_L. As shown in Fig. 6, the P_L value was proportional to the $\Delta C_p(T_g)$ value, and was considered to be a useful measure of amorphous FLF remaining in the solid dispersions.

Figure 7 shows the time profiles of the P_L values for FLF solid dispersions containing 20% (w/w) PVP or HPMC at 60 °C. The decrease in the ratio of Lorentzian fluorine atoms was faster for HPMC solid dispersions than for PVP solid dispersions, indicating that the overall crystallization rate of FLF in HPMC solid dispersions is larger than that in PVP solid dispersions. The overall crystallization rate depends on both molecular mobility (the rate of diffusion across the interface between crystalline and amorphous phase) and ther-

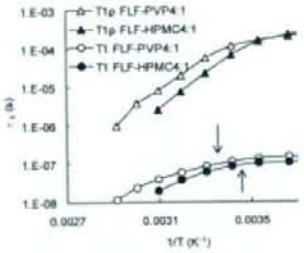

Fig. 3. Temperature Dependence of τ_c of FLF Fluorine Atoms in PVP and HPMC Solid Dispersions
Arrows in the figure represent T_g

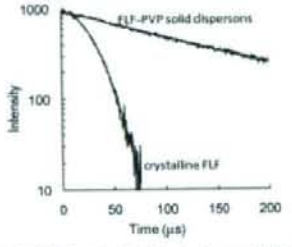

Fig. 4. Typical Solid Echo Signal of Fluorine Atoms of FLF in the Freshly Prepared Solid Dispersion Containing 20% (w/w) PVP and That of Fluorine Atoms of Crystalline FLF

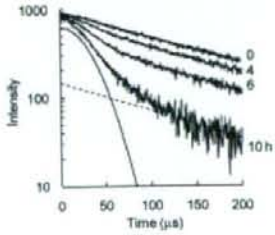

Fig. 5. Typical Solid Echo Signals of Fluorine Atoms of FLF in the Solid Dispersions Containing 20% (w/w) PVP Stored at 60 °C

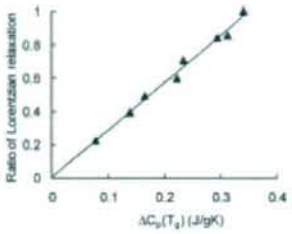

Fig. 6. The Ratio of FLF Fluorine Atoms Exhibiting Lorentzian Relaxation as a Function of Changes in the Heat Capacity at T_g

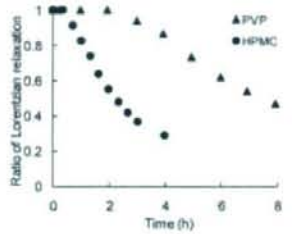

Fig. 7. Time Profiles of the Ratio of FLF Fluorine Atoms Exhibiting Lorentzian Relaxation in PVP and HPMC Solid Dispersions Stored at 60 °C

modynamic factors, such as free energy difference between crystalline and amorphous form.[2,3,10] Differences in the overall crystallization rate of amorphous FLF are consistent with those in the molecular mobility (Fig. 3), suggesting that the molecular mobility as determined by the ^{19}F-NMR spin–lattice relaxation times may be one of the factors determining crystallization rate, and useful as a measure of the physical stability of FLF in solid dispersions. The T_g values of the solid dispersions containing 20% PVP and 20% HPMC were 23 °C and 15 °C, respectively, indicating that molecular mobility reflected on T_g is higher for the solid dispersion containing HPMC than for that containing PVP. The T_g data seem to support the speculation obtained from NMR data. However, the scale of molecular mobility reflected on T_g is considered to be larger than that reflected on τ_c. Further studies should be conducted to elucidate the quantitative correlation between the physical stability of amorphous FLF and the molecular mobility determined by ^{19}F-NMR.

In conclusion, ^{19}F-NMR is useful for elucidating the molecular mobility of drugs containing fluorine atoms in amorphous solid dispersions. τ_c values of FLF fluorine atoms were calculated from the ^{19}F-NMR spin–lattice relaxation data. The τ_c value for solid dispersions containing 20% PVP was 2—3 times longer than that for solid dispersions containing 20% HPMC at 50 °C. Molecular mobility of FLF in the solid dispersions containing 20% PVP was lower than in those containing 20% HPMC, and this was consistent with the fact that the overall crystallization rate of amorphous FLF in the solid dispersion containing PVP was smaller than in that containing HPMC. The molecular mobility determined by ^{19}F-NMR seems to be useful as a measure of the physical stability of an amorphous drug in solid dispersions.

Acknowledgements Part of this work was supported by a Grant-in-aid for Research on Publicly Essential Drugs and Medical Devices from The Japan Health Sciences Foundation.

References

1) Yoshioka M., Hancock B. C., Zografi G., *J. Pharm. Sci.*, **84**, 983—986 (1995).
2) Matsumoto T., Zografi G., *Pharm. Res.*, **16**, 1722—1728 (1999).
3) Crowley K. J., Zografi G., *Pharm. Res.*, **20**, 1417—1422 (2003).
4) Shamblin S. L., Huang E. Y., Zografi G., *J. Therm. Anal.*, **47**, 1567—1579 (1996).
5) Shamblin S. L., Zografi G., *Pharm. Res.*, **16**, 1119—1124 (1999).
6) Zeng X. M., Martin G. P., Marriott C., *Int. J. Pharm.*, **218**, 63—73 (2001).
7) Miyazaki T., Yoshioka S., Aso Y., Kojima S., *J. Pharm. Sci.*, **93**, 2710—2717 (2004).
8) Khougaz K., Clas S., *J. Pharm. Sci.*, **89**, 1325—1334 (2000).
9) Berggren J., Alderborn G., *Eur. J. Pharm. Sci.*, **21**, 209—215 (2004).
10) Aso Y., Yoshioka S., Kojima S., *J. Pharm. Sci.*, **93**, 384—391 (2004).
11) Miyazaki T., Yoshioka S., Aso Y., *Chem. Pharm. Bull.*, **54**, 1207—1210 (2006).
12) Konno H., Taylor L. S., *J. Pharm. Sci.*, **95**, 2692—2705 (2006).
13) Aso Y., Yoshioka S., *J. Pharm. Sci.*, **95**, 318—325 (2006).
14) Harris R. K., Monti G. A., Holstein P., "Solid State NMR of Polymers," Chap. 6, ed. by Ando I., Asakura T., Elsevier, Amsterdam, 1998, pp. 351—414.
15) Grage S. L., Ulrich A. S., *J. Magn. Reson.*, **146**, 81—88 (2000).
16) Urano S., Matsuo M., Sakanaka T., Uemura I., Koyama M., Kumadaki I., Fukuzawa K., *Arch. Biochem. Biophys.*, **303**, 10—14 (1993).
17) Afonin S., Glaser R. W., Berditchevskaia M., Wadhwani P., Gührs K. H., Möllmann U., Perner A., Ulrich A. S., *ChemBioChem*, **4**, 1151—1163 (2003).
18) Salgado J., Grage S. L., Kondejewski L. H., Hodges R. S., McElhaney R. N., Ulrich A. S., *J. Biomol. NMR*, **21**, 191—208 (2001).
19) Williams S. P., Haggie P. M., Brindle K. M., *Biophys. J.*, **72**, 490—498 (1997).
20) Quint P., Ayala I., Busby S. A., Chalmers M. J., Griffin P. R., Rocca J., Nick H. S., Silverman D. N., *Biochemistry*, **45**, 8209—8215 (2006).
21) Farrar T. C., Becker E. D., "Pulse and Fourier Transform NMR," Academic Press, New York and Lodon, 1971.
22) Namgoong H., Lee J. W., *Bull. Korean Chem. Soc.*, **14**, 91—95 (1993).
23) Huang S.-G., Rogers M. T., *J. Chem. Phys.*, **68**, 5601—5606 (1978).
24) Gutowsky H. S., Lawrenceson I. J., Shimomura K., *Phys. Rev. Lett.*, **6**, 349—351 (1961).
25) Beckmann P. A., Rosenberg J., Nordstrom K., Mallory C. W., Mallory F. B., *J. Phys. Chem. A*, **110**, 3947—3953 (2006).
26) Horii F., "Solid State NMR of Polymers," Chap. 3, ed. by Ando I., Asakura T., Elsevier, Amsterdam, 1998, pp. 51—82.
27) Ruan R. R., Chen P. L., "Water in Foods and Biological Materials," Chap. 7, Technomic Publishing Co., Lancaster Basel, 1998, pp. 253—278.

Wide-Ranging Molecular Mobilities of Water in Active Pharmaceutical Ingredient (API) Hydrates as Determined by NMR Relaxation Times

SUMIE YOSHIOKA, YUKIO ASO, TSUTOMU OSAKO, TORU KAWANISHI

National Institute of Health Sciences, 1-18-1 Kamiyoga, Setagaya-ku, Tokyo 158-8501, Japan

Received 10 October 2007; revised 27 November 2007; accepted 28 November 2007

Published online 6 February 2008 in Wiley InterScience (www.interscience.wiley.com). DOI 10.1002/jps.21294

ABSTRACT: In order to examine the possibility of determining the molecular mobility of hydration water in active pharmaceutical ingredient (API) hydrates by NMR relaxation measurement, spin–spin relaxation and spin–lattice relaxation were measured for the 11 API hydrates listed in the Japanese Pharmacopeia using pulsed ^{1}H-NMR. For hydration water that has relatively high mobility and shows Lorentzian decay, molecular mobility as determined by spin–spin relaxation time (T_2) was correlated with ease of evaporation under both nonisothermal and isothermal conditions, as determined by DSC and water vapor sorption isotherm analysis, respectively. Thus, T_2 may be considered a useful parameter which indicates the molecular mobility of hydration water. In contrast, for hydration water that has low mobility and shows Gaussian decay, T_2 was found not to correlate with ease of evaporation under nonisothermal conditions, which suggests that in this case, the molecular mobility of hydration water was too low to be determined by T_2. A wide range of water mobilities was found among API hydrates, from low mobility that could not be evaluated by NMR relaxation time, such as that of the water molecules in pipemidic acid hydrate, to high mobility that could be evaluated by this method, such as that of the water molecules in ceftazidime hydrate.
 J Pharm Sci 97:4258–4268, 2008

Keywords: NMR relaxation time; dynamics; hydrate; DSC; water vapor sorption isotherm

INTRODUCTION

Correlations between chemical stability and molecular mobility have been demonstrated for various amorphous pharmaceuticals in the solid state.[1] Furthermore, the chemical stability of active pharmaceutical ingredient (API) hydrates is suggested to be correlated with the molecular mobility of water of hydration present in the crystalline structure.[2,3]

Water molecules in API hydrates exhibit a variety of physical states,[4,5] suggesting a range of molecular mobilities; water molecules incorporated into rigid crystalline structures may have low molecular mobility, whereas less rigid structures contain water molecules with greater mobility. Hydration water plays an important role in determining the physical characteristics—such as solubility[6] and flowability—of the API hydrate. Therefore, an understanding of the physical properties of hydration water, such as molecular mobility, is critical in the formulation of API hydrates.

The molecular mobility of water in solids may be determined by various methods, such as dielectric relaxation spectroscopy[7] and FT-Raman

Correspondence to: Sumie Yoshinka (Telephone: 81-3-3700-8547; Fax: 81-3-3707-6950; E-mail: yoshioka@nihs.go.jp)

Journal of Pharmaceutical Sciences, Vol. 97, 4258–4268 (2008)

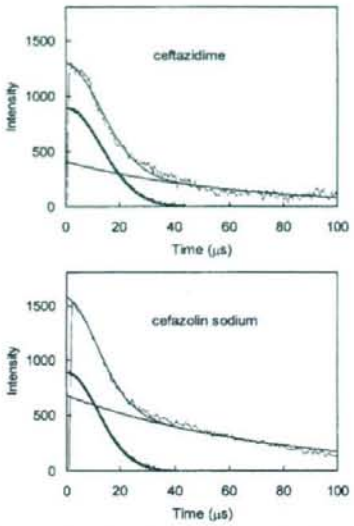

Figure 1. Free induction decay for ceftazidime and cefazolin sodium hydrates.

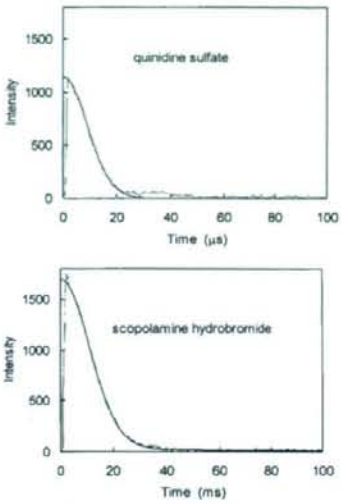

Figure 2. Free induction decay for quinidine sulfate and scopolamine hydrobromide hydrates.

spectroscopy.[8] NMR is also utilized to determine the molecular mobility of water in the solid state,[9] and to examine the various mechanisms by which solids interact with water.[10,11] However, there have been few studies in which the molecular mobility of water in API hydrates was determined using NMR. This may be because ^{1}H-NMR, even high resolution ^{1}H-NMR, cannot separate the peaks of the water protons from those of the protons in other components, which prevents specific determination of water mobility. Although the preparation of API hydrate samples using ^{17}O-labeled water allows to specifically determine the mobility of the water molecules by ^{17}O-NMR, unaffected by the other components, this approach requires high cost and much labor.

Table 1. Water Content of API Hydrates

API Hydrate	Number of H_2O per Molecule Specified in JP	Number of H_2O per Molecule Determined by KF	Spin–Spin Relaxation of H_2O
Cefazolin sodium	5	4.67	Lorentzian
Ceftazidime	5	5.04	Lorentzian
Amoxicillin	3	2.94	Lorentzian
Ampicillin	3	2.96	Lorentzian
Berberine Chloride	Not specified	2.67	Gaussian
Quinine hydrochloride	2	1.31	Gaussian
Scopolamine hydrobromide	3	2.32	Gaussian
Saccharin sodium	2	1.15	Gaussian
Pipemidic acid	3	2.9	Gaussian
Sulpyrine	1	0.98	Gaussian
Quinidine sulfate	2	1.95	Gaussian

DOI 10.1002/jps